processes

MDPI

Article

Influence of Varying Compression Ratio of a Compression Ignition Engine Fueled with B20 Blends of Sea Mango Biodiesel

R Rohith Renish [1], Amala Justus Selvam [2], Robert Čep [3,*] and Muniyandy Elangovan [4,*]

[1] Department of Mechanical Engineering, Vel Tech Rangarajan Dr. Sagunthala R&D Institute of Science and Technology, Chennai 600062, Tamil Nadu, India; rohith.renish@gmail.com
[2] Department of Automobile Engineering, Vel Tech Rangarajan Dr. Sagunthala R&D Institute of Science and Technology, Chennai 600062, Tamil Nadu, India; amalajustus@gmail.com
[3] Department of Machining, Assembly and Engineering Metrology, Faculty of Mechanical Engineering, VSB-Technical University of Ostrava, 708 00 Ostrava, Czech Republic
[4] Department of R&D, Bond Marine Consultancy, London EC1V 2NX, UK
* Correspondence: robert.cep@vsb.cz (R.Č.); muniyandy.e@gmail.com (M.E.)

Abstract: The ever-worsening environmental situation brought on by the huge use of fossil fuels has ramped up biodiesel production. Several studies have shown that a 20% biodiesel-diesel blend (B20) could be the best for utility in a compression ignition (CI) engine. The present study focuses on the characteristics of a variable compression ratio (VCR) engine running with a B20 blend of sea mango biodiesel at compression ratios of 16:1, 17:1 and 18:1. VCR is a technology which permits the engine to modify its compression ratio to improve the fuel economy under varying loads. The experimental results reveal an improvement of 5.27% and 6.25% in the BTE as well as SFC with B20 mix, respectively, at compression ratio (CR) 18:1 against diesel at standard CR, which is 17:1. At CR 18:1, the CO, HC and smoke emissions of B20 fuel at full load were 26.78%, 37.76% and 23.44%, correspondingly lower than those of diesel at standard CR. However, the blend was found to have higher NO_x emissions at all the CRs. The least NO_x emissions of the blend were noted to be at CR 16:1, although it was 0.77% higher than diesel at standard CR. The combustion characteristics also improved at higher CRs. The findings of this study indicate that the B20 blend of sea mango biodiesel could be utilized at CR 18:1 to replace diesel without any engine modifications.

Keywords: sea mango biodiesel; B20; VCR engine; engine characteristics; emissions; compression ratio

Citation: Renish, R.R.; Selvam, A.J.; Čep, R.; Elangovan, M. Influence of Varying Compression Ratio of a Compression Ignition Engine Fueled with B20 Blends of Sea Mango Biodiesel. *Processes* **2022**, *10*, 1423. https://doi.org/10.3390/pr10071423

Academic Editor: Blaž Likozar

Received: 10 July 2022
Accepted: 19 July 2022
Published: 21 July 2022

1. Introduction

Energy plays a vital factor in day-to-day life. Every essential amenity in the current context is dependent on energy. The energy demand has been rapidly increasing as a result of industrialization [1]. Following the invention of internal combustion engines, the world's need for oil-based fuels drastically increased. Fossil fuels are considered to be the most important source in the operation of thermal power plants, generators and vehicles [2]. The over-usage of fossil fuels has resulted in vast volumes of carbon and nitrogen oxides being spewed into the atmosphere, with levels rising at an alarming rate. As a result of both the depletion of fossil fuels and the pollutants they produce, specialists have begun searching for sustainable alternatives [3]. Biodiesel is considered to be one of the finest alternatives to substitute petroleum diesel due to its characteristics such as renewable, decreased emissions; great combustion performance; biodegradability; and improved lubrication [4–10]. Biodiesels are sustainable fuels generated from triglycerides by the transesterification process [11]. Biodiesel research has recently accelerated, and many experts believe that biodiesel generated from a variety of feedstocks may be used as a viable alternative to traditional diesel fuel [12]. Many experts have obtained better efficiencies and improved emissions characteristics when CI engines run with biodiesel

blends. However, a modest rise in nitrogen oxide (NO_x) emission was always seen due to a large increase in temperatures during the combustion process. To address this issue, numerous scholars have resorted to researching impacts by altering engine settings such as injection timing, injection pressure and compression ratios (CRs).

In diesel engines, the compression ratio is determined by comparing the greatest volume of the combustion chamber at the bottom dead center (BDC) piston position to the lowest volume at top dead center (TDC). It provides control of peak cylinder pressure and improves cold start ability and low load operation, enabling the multi-fuel capability, increase in fuel economy and reduction in emissions.

There are several advantages of using a VCR engine:

1. Low exhaust emissions and fuel consumption.
2. Most efficient burning of fuel at all speeds and loads.
3. The VCR engines have great fuel flexibility.
4. Its thermal efficiency is better than that of fixed compression ratio engines.
5. The VCR gives better control over pollutant production and cleanup than a fixed compression ratio.
6. It results in low vibration levels and permits a large drop in idle speed due to decreased misfiring and cycle abnormalities.
7. By allowing the catalytic converter's catalyst to warm up early, cold starting emissions may be significantly minimized.
8. Effective idling at low ambient temperatures.
9. An increase in low-end torque from a gasoline engine without the danger of detonation.
10. Recurring frictional losses as a result of almost constant peak pressures.
11. The VCR engine operates at the optimal compression ratio for compressed natural gas or gasoline. Bi-fuel cars may employ VCR engines. It has several fuel possibilities and high combustion efficiency.
12. VCR engines can also provide the highest possible combustion efficiency.

Today, automakers invest billions on green cars. To keep the environment clean, automobile manufacturers are investing heavily in R&D. The firm is exploring techniques to reduce automobile emissions and manufacture eco-friendly cars.

Honda Company Ltd. (Tokyo, Japan) showed the World Congress documentation on their variable compression ratio engine research. They designed a small VCR that uses piston inertia to vary compression levels (Concept: Honda R&D Developing Variable Compression Ratio Engine with Dual Piston Mechanism, 2009). SAAB is developing a new, efficient VCR engine. SAAB criticized their SVC (Saab Variable Compression) engine at the Geneva Motor Show. The new fuel-efficient idea was revolutionary. Reduced engine displacement and a novel system of variable compression ratio improved the engine's performance. Fuel usage and carbon emissions were moted to decrease by 30%. The SVC engine system prevented external or internal friction from increasing engine losses. Nissan has developed a piston-crank mechanism that enables variable engine compression, unlike other automobiles' static compression. The technology optimizes engines' rpm with compression ratio and may change with vehicle speed, resulting in optimal combustion and higher power and fuel efficiency (Nissan). This shows that the automobile industry is searching for novel methods to boost the future vehicle market and the environment.

Several studies have been done using VCR engine with various feedstocks. Navdeep Sharma et al. [13] examined the characteristics of dual biodiesel blend, mahua and jatropha at equal proportions with diesel in a diesel engine with various CRs of 13.5:1, 14.5:1, 15.5:1 and 16.5:1. The brake power (BP) and mechanical efficiency (ME) of the blends improved by 0.15–1.58% and 1.07–12.42%, respectively, compared to diesel at CR 16.5:1. The peak cylinder pressure (Cp) and exhaust gas temperature (EGT) of the blends were found to be 0.15–0.36 bar and 11.1–69.8 °C lower than mineral diesel, respectively. The CO and HC emissions of the blends were lowered by 33–62%. Among all the blends, blend B20 was indicated to be the most effective. Areef Ahamed et al. [14] studied the impact of CRs 18:1, 20:1 and 22:1 as well as EGR rates of the diesel engine run on B20 blend of mango seed

methyl ester. At CR 22:1, the brake thermal efficiency (BTE) increased by 7.4%, reducing the emissions of CO, HC and smoke by 33.3%, 40% and 7.1%, respectively. The amount of NO_x emitted increased significantly. The engine running at CR 22:1 with 5% EGR reduced NO_x emissions by 40.5%. Pali Rosha et al. [15] evaluated the impacts of CRs 16:1, 17:1 and 18:1 in a CI engine utilizing 20% of palm oil biodiesel blend. The ignition delay (ID) period decreased while the Cp and BTE rose at higher CR. The blend exhibited a maximum BTE of 33.8% at 3.5 brake mean effective pressure and 18:1 CR. The rise in CR from 16:1 to 18:1 also resulted in an average reduction of 47.8%, 41.0% and 35.7% in the emissions of HC, CO and smoke opacity, respectively, but with an increase of 41.1% in the NO_x. Suresh et al. [16] studied the characteristics of argemone mexicana methyl ester (AME) and its blends in a carriable compression ratio (VCR) engine at CRs varying from 14:1 to 18:1. In comparison to diesel and other blends, the AME20 at CR 17:1 resulted in greater BP, BTE and improved specific fuel consumption (SFC). With a modest rise in NO_x, the HC and CO emissions also improved. K. Sivaramakrishnan et al. [17] evaluated the characteristics for a VCR engine fueled with 20%, 25% and 30% of karanja biodiesel-diesel blends at CRs 15:1, 16:1, 17:1 and 18:1. The B25 blend at CR 18:1 revealed the maximal BTE to be 30.46%. As the blend ratio grew, the emissions of HC and CO decreased. At higher CRs, the combustion pressure of the blends improved. 18:1 was proven to be the greatest effective CR. Datta et al. [18] performed tests on a diesel engine with CRs ranging from 16:1 to 18:1. The BTE of clean palm oil biodiesel was noted to be 7.9% lower than that of diesel but increased with CR. Heat release rate falls with biodiesel, reaching a nadir at the rated CR of 17.5:1. In contrast, with neat diesel, the inflammatory delay has been more severe and rises as the compression ratio decreases. Lowering the CR resulted in increases in CO, HC and smoke emissions of the palm oil biodiesel but decreased the NO_x and CO_2 emissions. Mohit Vasudeva et al. [19] evaluated the impact of CRs 15:1, 16:1, 17:1 and 18:1 of a CI engine when run with 10% to 40% of a rice bran biodiesel-diesel blend. The increase in CR from 15:1 to 18:1 led to an average reduction in brake-specific fuel consumption (BSFC) of 18.6% and improved the BTE by 14.66%. The CO and HC emissions were lowered by 22.27% and 38.4%, but increased the CO_2 and NO_x emissions by 17.43% and 22.76%, respectively, as the CR rose from 15:1 to 18:1. The increase in CR also resulted in a 15% rise in the Cp. Bora et al. [20] conducted experiments on raw biogas at three different CRs (18:1, 17.5:1 and 17:1) and an injection timing of 23° bTDC. At CRs 18:1,17.5:1 and 17:1 and full load, it had the highest BTEs of 20.27%, 19.97% and 18.39%, correspondingly. The highest liquid fuel replacement (LFR) was 80%, 79% and 78.2% at CRs 18:1,17.5:1 and 17:1, respectively. When the CR was raised from 17:1 to 18:1, the CO and HC emissions dropped by 17.67% and 17.18%, respectively, but the NO_x emissions raised by 42.85%. A study by Sharma et al. [21] looked at how changing the CR of a CI engine could affect its behavior. Two different CRs were used in the study, 16.5:1 and 18.5:1. Compared to the original CR, the enhanced CR of 18.5:1 resulted in shorter ID, maximum Cp and faster heat release rate (HRR). As compared to the initial CR, raising the CR from 17.5:1 to 18.5:1 improved the BTE by about 8%. With a CR of 18.5:1, the blend produced 10.5%, 32% and 17.4% lesser BSCO, BSHC and smoke opacity, respectively. Bora et al. [22] investigated a study using raw biogas under various loading at CRs 18:1, 17.5:1 and 17:1. The maximum BTE were determined to be 20.27%, 19.97% and 18.39% at CRs of 18:1, 17.5:1 and 17:1, respectively. The maximum LFR for the same parameters were determined to be 80%, 79% and 78.2% for CRs of 18:1, 17.5:1 and 17:1, respectively. The CO and HC emissions were reduced by 17.8% and 17.2%, respectively, as the CR was raised from 17:1 to 18:1. However, the same CR also resulted in an increase of 14.13% CO_2 and 42.85% NO_x emissions. Mohammed EL et al. [23] investigated the impact of CRs 14:1, 16:1 and 18:1 on waste oil biodiesel blends B10 to B50. Higher CRs improved both the BSFC as well as the BTE. The CO and HC emissions dropped by 37.5% and 52%, whereas NO_x and CO_2 emissions grew by 36.8% and 14.3%, respectively. Despite having lower volatility and higher viscosity than diesel, biodiesel appears to have a shorter igniting delay. Muralidharan et al. [24] studied the effect of CR in a VCR engine when run with waste sunflower oil biodiesel blends at different CRs ranging from 18:1 to 22:1. The

increase in the CR improved combustion efficiency, and caused longer ignition delays and higher maximum rate of pressure increase than diesel. The maximum BTE was obtained with the blend B40. The blend lowered the HC and CO emissions as well, but increased the NO_x. Suresh et al. [25] reviewed the work of several authors with biofuels on VCR engines and indicated the fact that the blends of biodiesel with diesel may be used directly in a VCR engine without any alterations on the engine. Several studies proved that the VCR engines resulted in higher engine performance and less emissions than diesel at higher CRs. However, due to high peak temperatures, there was a minute rise in NO_x emissions. The authors conclude that the VCR engines have the potential to improve the combustion efficiency of the fuel.

Previous studies show that the use of biodiesel from various feedstocks can enhance the emission properties with a modest decrease in their performance. Several research experiments have been undertaken to improve the performance and minimize emissions through several ways, such as using pure biodiesel, blending biodiesels in different proportions with diesel, varying the compression ratios of an engine, fuel supply and combustion chamber modifications and addition of nano additives.

High compression ratios could be ideal for engine operation. Unfortunately, high compression produces more heat, which sometime promotes detonation—when the air-fuel combination suddenly bursts before the spark plug fires—which may cause slight damage to the engines. Engineers have traditionally had to decide between high compression with moderate boost and low compression with strong boost because turbocharged engines operating at high boost levels are particularly sensitive to detonation, and this could be one of the reasons why the VCR engines did not get much attention. At the same time, however, many researchers have also showed that higher compression ratios result in better engine characteristics.

Several scientists have proved that B20 is the optimal biodiesel blend that can be used in a CI engine [26–35]. Although several works have been carried out using diverse feedstocks, only a few have focused on sea mango oil [36], which has encouraged the authors to work on the B20 blend of sea mango biodiesel at different CRs.

There have been a few studies on sea mango, which were mainly concerned with its toxicity. In this study, the VCR engine was run with B20 (20% sea mango biodiesel + 80% diesel) biodiesel blend for evaluating its engine characteristics at different CRs. The uniqueness of this work stems from the fact that no similar studies have been published on sea mango biodiesel so far. Experiments were done at 1500 rpm with varied loading circumstances ranging from 0 to 12 kg for different CRs of 16:1, 17:1 and 18:1.

2. Materials and Methods

2.1. Overview of Sea Mango

Sea mango, also known as Cerbera odollam [37] or Cerbera manghas [38], is said to be a poisonous tree which belongs to the Apocynaceae family [39]. These are evergreen trees that grow 6–15 m high with luminous dark green spiral-like leaves with egg-shaped fruits of 5–10 cm in length and are commonly found in the coastal areas of South India, Malaysia, the riverbanks of Vietnam, Sir Lanka, Madagascar and Myanmar. These trees are highly poisonous due to the high concentration of cerberin heart glycoside in their fruit and leaves. In Kerala, India, there have been several cases of sea mango seeds being used as suicide poison [40]. Sea mango is a relatively fresh and unknown non-edible fruit.

2.2. Fuel Preparation

The sea mango biodiesel was prepared by the esterification and transesterification methods using sea mango oil at the Indian Biodiesel Corporation (IBDC), Baramati. It was necessary to undergo the two-step method for producing biodiesel due to the high FFA (free fatty acid) value of sea mango oil. To decrease the acid value of the feedstock oil, acid esterification was initially carried out with an 8:1 molar ratio of methyl alcohol to oil for 90 min with 1.5% sulfuric acid as an acid catalyst. To circumvent the mass transfer

restriction, the mechanical stirrer's speed was maintained constant at 600 rpm. After the acid-esterification process, the reaction mixture was allowed to settle for 4 h. The esterified sea mango oil was then subjected to the transesterification reaction to complete the process. As a solid base heterogeneous catalyst, CaO was utilized in this study. The process took place with a 10:1 molar ratio of alcohol to oil, with 3% CaO at a temperature of 65 °C for 120 min. Two different layers were observed after allowing the reaction to settle at the end. The glycerol layer was drawn out, and the methyl ester was collected and transferred to the washing process to produce pure biodiesel. The properties of the fuel samples are listed in Table 1 as defined by ASTM standards.

Table 1. Fuel test properties.

Fuel Properties	Unit	Diesel	B20	B100	ASTM Test Method [41]	Limit
Calorific Value	MJ/kg	42.5	42.08	38.62	D240	34–45
Cetane No	-	49.22	49.77	51.71	D613	>47
Viscosity at 40 °C	mm^2/s	2.7	2.96	4.2	D445	1.9–6
Density at 15 °C	g/cm^3	0.831	0.839	0.875	D1298	0.8–0.9
Fire Point	°C	71	83	156	D93	140–215
Flash Point	°C	64	86	142	D93	>130
Cloud Point	°C	−4.0	−2.1	7.2	D2500	−3 to 12

2.3. Experimental Setup

The experiments were performed using a single-cylinder, four-stroke VCR engine powered by B20 blend of sea mango biodiesel. Table 2 lists the major features of the VCR engine. The VCR engine is designed in such a way that the CR could be varied even without halting the engine. To measure the movement of the cylinder, a micrometer is attached to the cylinder. Two piezo-type sensors are installed on the fuel injector and cylinder head to direct the fuel line and combustion pressure. Two K-type thermocouples and four PT100 type thermocouples are installed throughout the setup to monitor the exhaust gas temperature. The fuel is measured using a differential pressure transducer. Rotameters were used to monitor the cooling water's flow for the cylinder head, engine block and calorimeter. The IC Engine soft v9.0 application is used to analyze the test rig's performance using all of the analog data collected from different points. In order to determine the amount of NO_x, HC, CO and smoke present in the engine's exhaust, AVL Digas 444N gas analyzer and the AVL 437 smoke meter were employed. The VCR engine's primary specifications are shown in Table 2. Table 3 displays the range, accuracy and uncertainties of instruments. The schematic layout of the engine arrangement is shown in Figure 1, and a photographic image of the test equipment is shown in Figure 2.

Table 2. Test engine details.

Parameter	Specification
General details	Multifuel, four-stroke, VCR engine
Ignition	Compression ignition
Compression ratio	12:1–18:1
Loading	Eddy current dynamometer
Speed	1500 rpm
Number of cylinders	1
Rated power	3.5 kW
Stroke	110 mm
Bore	87.5 mm
Air flow transmitter	Pressure transmitter
Temperature sensor	Type K, PT100 thermocouple
Rotameter	Calorimeter 25–250 LPH
Cooling	Water-cooled

Table 3. Range, accuracy and uncertainty of the instruments.

Equipment	Measured Quantity	Accuracy	Measuring Range	Uncertainty
AVL Digas 444N gas analyzer	O_2	±5%vol	0–22%vol	±0.5%
	HC	±5 ppm	0–20,000 ppm	±0.4%
	CO_2	±0.5%vol	0–20%vol	±0.3%
	CO	±0.03%vol	0–10%vol	±0.15%
	NO_x	±10 ppm	0–5000 ppm	±1.2%
AVL 365C angle encoder	Crank angle	±1 °CA	0–720 °CA	±0.5%
AVL 437 smoke meter	Smoke	±2%	0–100%	±0.8%
Tachometer	Engine speed	±5 rpm	1–10,000 rpm	±0.2%
DP fuel flow transmitter	Fuel flow rate	±2 mmWC	0–500 mmWC	±0.5%
Thermocouple	Exhaust gas temperature	±2 °C	0–1200 °C	±0.2%
AVL GH14D pressure transducer	Pressure	±0.3 bar	0–250 bar	±0.25%

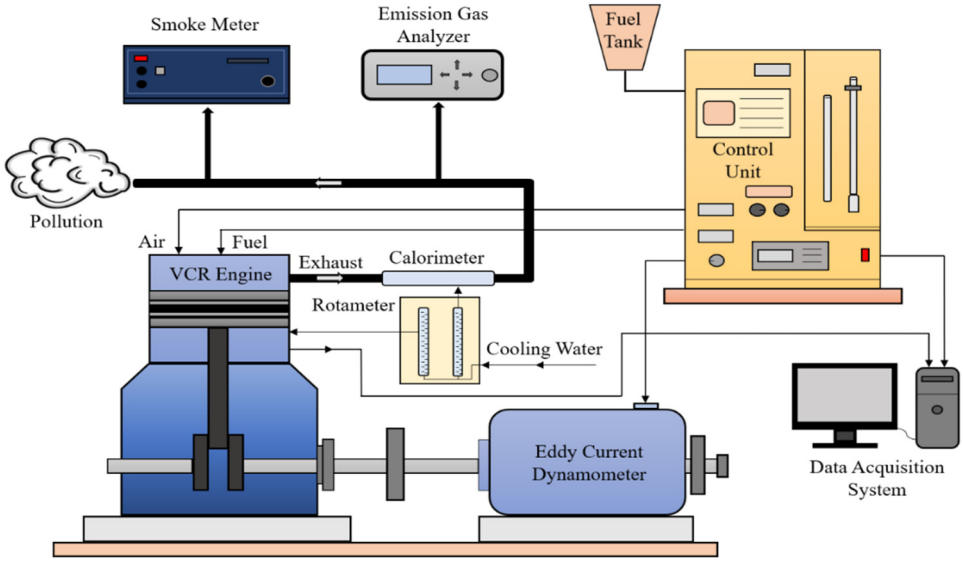

Figure 1. Schematic representation of the engine's layout.

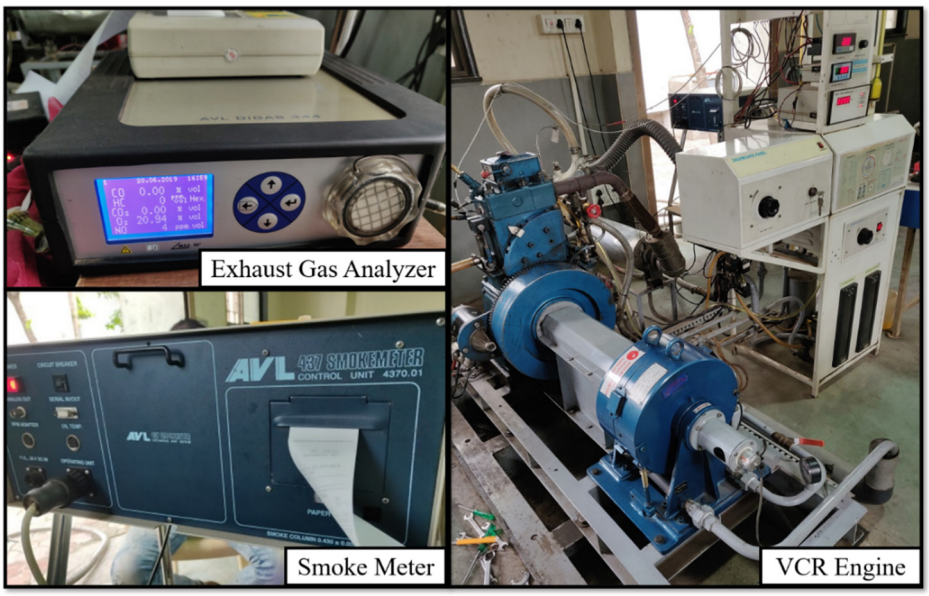

Figure 2. Photographic images of the testing equipment.

2.4. Uncertainty Analysis

Uncertainty analysis is done to calculate errors of various parameter measurements. Every set of tests was replicated thrice to validate the consistency of their results. The uncertainty proportion for each measurement is shown in Table 4. The following formula was used to compute the total uncertainty:

$$= \sqrt{\begin{array}{c}(\text{BTHE})^2 + (\text{SFC})^2 + (\text{EGT})^2 + (\text{CO})^2 + (\text{HC})^2 + (\text{NO}_x)^2 + (\text{Smoke})^2 + \\ (\text{CP})^2 + (\text{HRR})^2\end{array}}$$

$$= \sqrt{\begin{array}{c}(0.75)^2 + (0.15)^2 + (0.75)^2 + (0.28)^2 + (0.72)^2 + (1.45)^2 + (0.82)^2 + \\ (0.25)^2 + (0.55)^2\end{array}}$$

$$= \pm 2.21$$

Table 4. The uncertainty percentage for various metrics.

Parameters	Uncertainty %
BTE	±0.75
SFC	±0.15
EGT	±0.75
HC	±0.72
CO	±0.28
NO_x	±1.45
Smoke	±0.82
Cylinder pressure (Cp)	±0.25
Heat release rate (HRR)	±0.55

3. Result and Discussion

A CI engine's behavior is influenced significantly by its compression ratio. For the first 30 min, the engine was allowed to operate on diesel fuel at full load to ensure that the exhaust gas and the outlet cooling water temperature were maintained at a constant level to achieve the steady-state condition. This signifies that the combustion within the cylinder has reached a stable state and the engine is prepared to gather data. The engine was then gradually reverted to a no-load state and operated for a few minutes. The investigation began with the collection of the engine's baseline findings while powered by diesel, varying its loads at regular intervals, which correspond to their respective brake power at CR 17:1. The other parameters such as speed, injection pressure and timing were maintained at 1500 rpm, 210 bar and 23° bTDC, respectively, throughout the experiment. Studies were conducted with sea mango B20 biodiesel blend at different CRs of 16:1, 17:1 and 18:1 and compared with that of diesel engine characteristics at 17:1 CR. The test findings are reported in the following sections.

3.1. Performance Analysis

3.1.1. Brake Thermal Efficiency

The efficiency of fuel energy conversion to useable work is predicted by brake thermal efficiency (BTE) [42]. Figure 3 illustrates the impact of CRs on the BTE for the fuel samples. There is a distinct rise in BTE as load increases due to lowered heat loss and increased power at higher loads [43]. The findings show that at standard CR (17:1), the BTE of diesel and B20 blend were obtained as 28.36% and 27.55%, respectively, at full load, which are fairly close to one other. It is conceivable that the low energy content of the mix is responsible for its lower BTE [14]. The increase in the compression ratio enhanced the engine's BTE. The BTE of B20 blend at full load was noted to be 26.21%, 27.55% and 29.94% at CRs 16:1, 17:1 and 18:1, respectively. In part, this improvement in BTE might be attributed to an increase in compressed air temperature, which leads to improved combustion of the blend at higher CRs [44]. The blend had the highest BTE of 29.94% at CR 18:1, which was 5.57% more than that of diesel at standard CR.

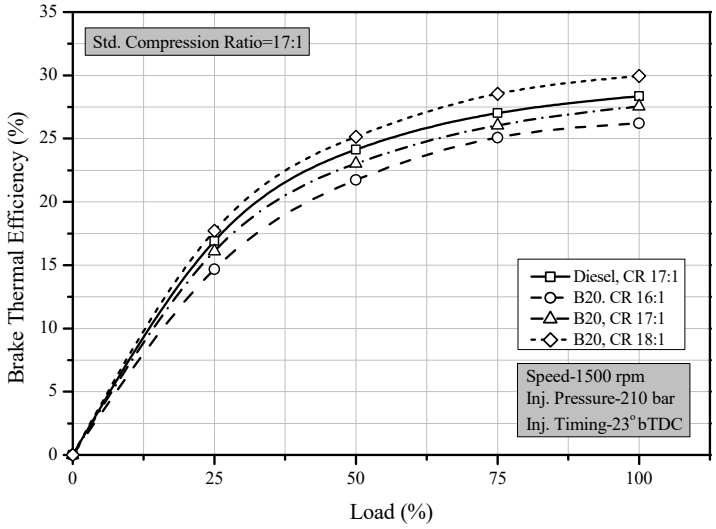

Figure 3. BTE vs. load at different CRs.

3.1.2. Specific Fuel Consumption

The specific fuel consumption (SFC) is the quantity of fuel used to produce one unit of brake power [42]. The fluctuation in SFC for the fuel samples at different CRs are shown in Figure 4. The SFC decreased dramatically from no load to part load and then gradually decreased as load increased. This is due to the fact that at higher loads, heat loss is lesser [45]. At standard CR, the SFC readings for diesel and the B20 blend were reported to be 0.32 and 0.34 kg/kWh, respectively. The blend has a slightly greater SFC than diesel owing to its lower heating value. However, due to the similar calorific value of the B20 blend and diesel, they are very close to one another [46]. The SFC of the blend at full load and CRs 16:1, 17:1 and 18:1 was recorded to be 0.37 kg/kWh, 0.34 kg/kWh and 0.3 kg/kWh, respectively. The SFC reduced with higher CRs. The reasonable factor for this tendency is that when CR rises, the maximum cylinder pressure increases as the outcome of the fuel being fed into a hotter combustion chamber, resulting in greater effective power [47]. The lowest SFC of the blend was identified to be 0.3 kg/kWh at CR 18:1, which showed an improvement of 6.25% over diesel at standard CR.

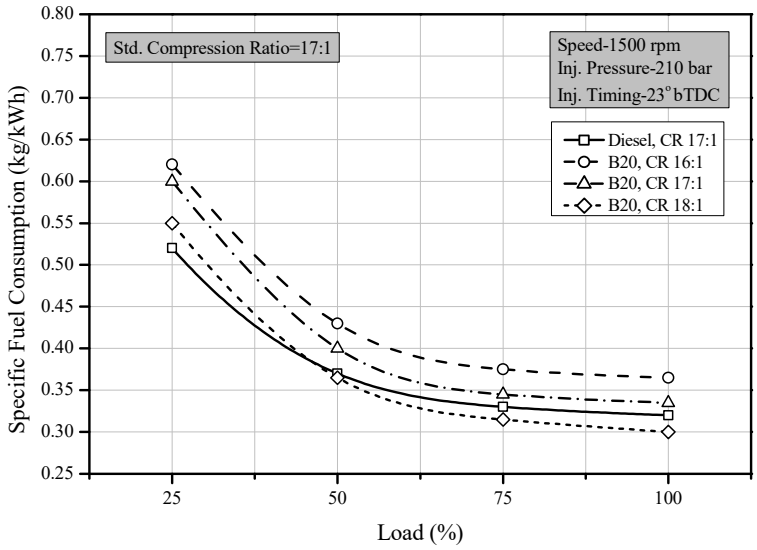

Figure 4. SFC vs. load at different CRs.

3.1.3. Exhaust Gas Temperature

The measure of heat emitted by the fuels during combustion can be referred to as exhaust gas temperature (EGT) [18]. Figure 5 depicts the variation in EGT for the fuel samples at different CRs. The EGT rises with the engine load, owing to a greater combustion temperature which takes place within the cylinder at higher loads [21]. The EGT for diesel and the B20 blend at the standard CR were 325 °C and 345 °C, respectively, at full load. Due to increased heat loss and decreased thermal efficiency, the biodiesel blend's exhaust gas temperature was higher than diesel [48]. At full load, the EGT of the blend was noted to be 364 °C, 345 °C and 338 °C at CRs of 16:1, 17:1 and 18:1, respectively. The drop in EGT at higher CRs may be due to increased expansion of burned gases and a larger quantity of work done by the burnt mixture. [49]. Increased air temperature, which aids in greater atomization of the fuel, results in complete combustion, which is also a reason for EGT reduction at higher CRs [21]. At CR 18:1 and full load, the blend's EGT was noted to be 338 °C, which was still 4% higher than diesel at standard CR.

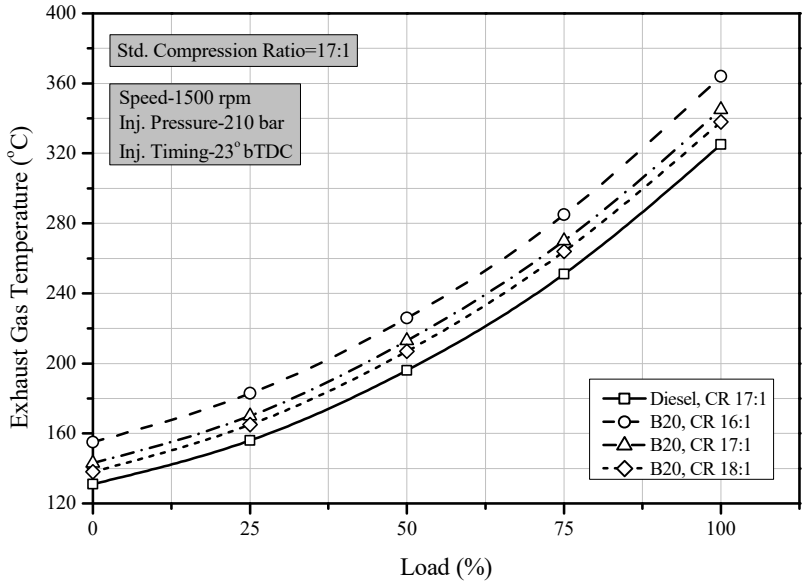

Figure 5. EGT vs. load at different CRs.

3.1.4. Comparative Analysis in Performance

Figure 6 depicts the percentage difference in the performance of the B20 blend at different CRs to diesel at standard CR and full load. The difference in BTE of the blend at CRs 16:1 and 17:1 was reduced by 7.58% and 2.85%, respectively, at full load, but rose to 5.57% at CR 18:1 compared to diesel. At maximum load, the SFC of the blend at CRs 16:1 and 17:1 was 14.06% and 4.68% higher than diesel, but was lowered by 6.25% at CR 18:1. The EGT at peak load was 12%, 6.15% and 4% higher than diesel at CR 16:1, 17:1 and 18:1, respectively. The performance of the blend with higher CRs was noticed to improve. This largely reflects the fact that fuel is more atomized with higher CRs, the compressed air temperature rises, and the enhanced fuel spray characteristics which contribute to complete combustion.

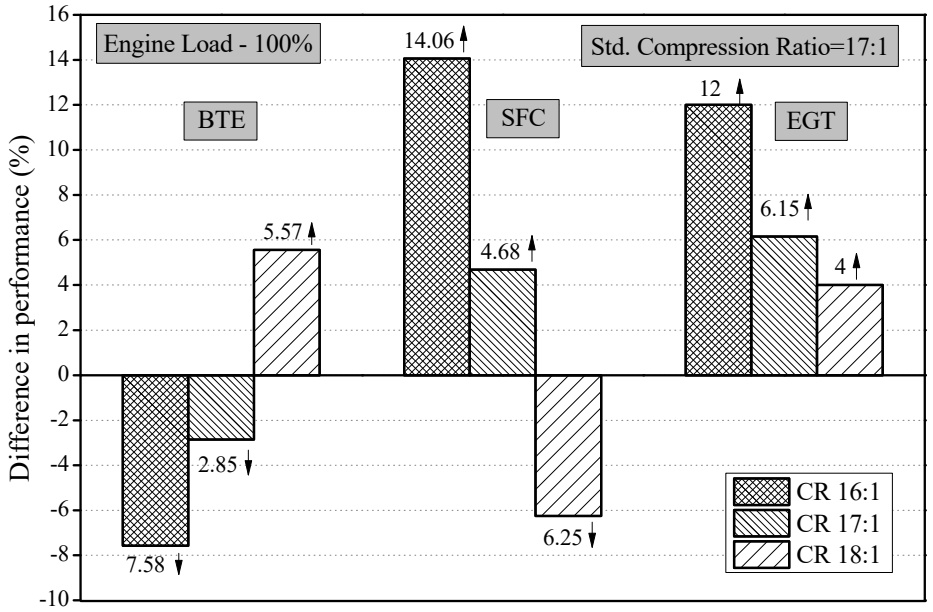

Figure 6. Percentage difference in performance of B20 blend at varying CRs to diesel at standard CR and full load.

3.2. Emission Characteristics

3.2.1. Carbon Monoxide

Carbon monoxide (CO) is produced when fuel in an engine is not completely burned. Incomplete combustion takes place if there is not enough oxygen present to complete the combustion [50]. Figure 7 shows the CO emissions of the fuel samples at various CRs. The CO emissions of the fuel samples decrease up to 60% load and subsequently increase. At low loads, the engine's gas temperature stays low, leading to incomplete combustion in the gas phase and very significant CO emissions. Due to the increased temperature of the gas within the cylinder, at higher loads, the CO oxidation rate rises, leading to reduced CO emissions. Under fully loaded conditions, the injected fuel is high and the fuel distribution becomes uneven. This leads to poor mixing and a high concentration of CO [43]. At the standard CR, the emissions of CO for diesel and the B20 blend at full load were 0.28% and 0.24%, respectively. Due to the higher oxygen concentration in the biodiesel blend, it emits less CO than diesel [47]. The CO emissions for the blend at CRs 16:1, 17:1 and 18:1 were 0.26%, 0.24% and 0.21%, respectively, at full load. The CO emissions of the blend dropped when the CR was raised. This is due to the fact that more air and oxygen are accessible within the cylinder for complete combustion to take place at higher CRs [49]. At CR 18:1, the blend generated the lowest CO emissions of 0.21%, which was 26.78% lower than the CO produced by the diesel at standard CR.

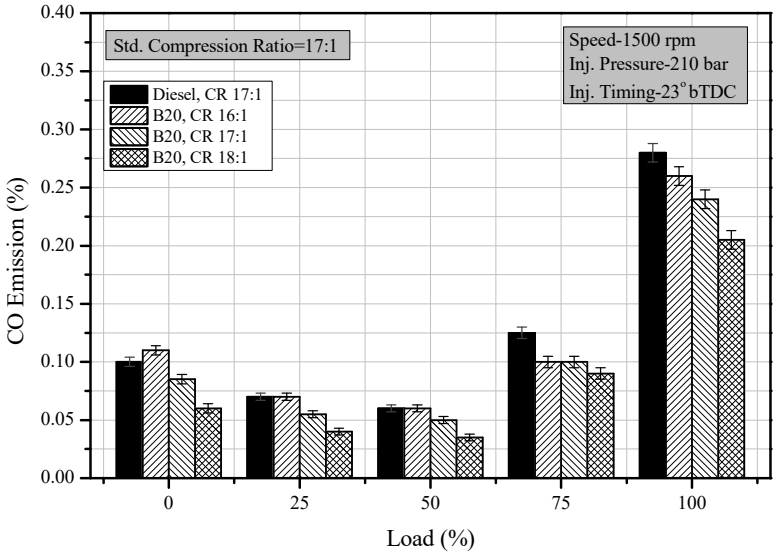

Figure 7. CO emissions vs. load at different CRs.

3.2.2. Hydrocarbons

Fuel entrapment in the combustion crevice, incomplete fuel evaporation, bulk quenching of the oxidation process at low temperatures, and locally lean or rich mixtures are all plausible causes of fuel's hydrocarbon (HC) emissions [51]. Figure 8 depicts the HC emission at different CRs for the fuel samples. The graph demonstrates that, as the load grew, HC emissions increased as well, owing to the existence of rich fuel blends and lower oxygen content for combustion at higher loads [52]. At standard CR, the HC emission for diesel and the B20 blend were 65 ppm and 54 ppm, respectively, at full load. The oxygen content in the blend interacts with the hydrocarbons present in the fuel, lowering its HC emission compared to diesel [43]. At CRs 16:1, 17:1 and 18:1, the HC of the blend were measured to be 58 ppm, 54 ppm and 45 ppm, respectively, at full load. It has been noticed that the HC emissions drop gradually when the CR is increased. At higher CRs, reduced HC emissions are achieved owing to the increase in air intake temperature at the end of the compression stroke, which raises the combustion temperature and leads to improved combustion [53]. The blend achieves a minimal HC emission of 45 ppm at CR 18:1, which was 37.76% lower than the diesel operated at standard CR and full load.

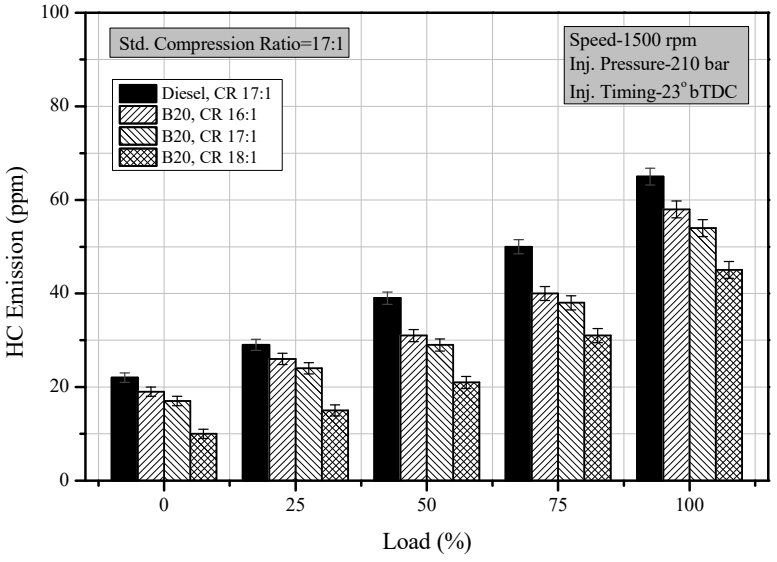

Figure 8. HC emissions vs. load at different CRs.

3.2.3. Oxides of Nitrogen

Temperature, oxygen content and time allotted for reactions to take place are the primary factors influencing nitrogen oxide (NO_x) emissions during premixed combustion [49]. The fuel samples' NO_x emissions at different CRs are shown in Figure 9. The NO_x emissions increased with respect to load due to the increase in the combustion temperature caused by high in-cylinder pressure at higher loads [43]. At standard CR, the NO_x emissions of diesel and the B20 blend were noted to be 1044 ppm and 1107 ppm, respectively, at full load. Blend's oxygen content raises the maximum gas temperature in the cylinder, which improves combustion and raises the NO_x concentration as well [47]. The NO_x also increased along with the CR. It was determined that, for CRs 16:1, 17:1 and 18:1, the blend's NO_x emission values at full load were 1052 ppm, 1107 ppm and 1193 ppm, respectively. The higher the CR, the higher the temperature within the combustion chamber due to the enhanced combustion resulting in increased NO_x emissions [53]. At full load, the B20 blend recorded its lowest NO_x of 1052 ppm at CR 16:1, as it reduces the pre-premixed heat release rate, causing a lower temperature of combustion [18]. The NO_x emission of the blend at CR 18:1 was 14.27% higher than diesel at standard CR.

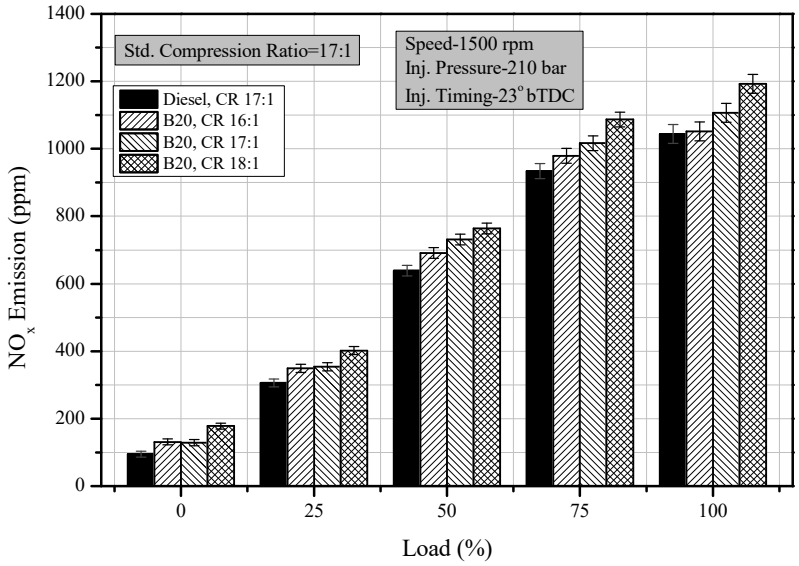

Figure 9. NO_x emissions vs. load at different CRs.

3.2.4. Smoke Opacity

Smoke is formed when lack of oxygen in the combustion zone prevents the fuel from being fully oxidized [18]. The results of smoke opacity at various CRs are shown in Figure 10. From the graph, it is evident that when the load rises, the smoke density also increases as the quantity of fuel injected increases at higher loads, resulting in rich mixture [54]. The smoke opacity of diesel and the B20 blend at standard CR was 67.4% and 57.2%, respectively, at full load. The blend produces less smoke than diesel because it contains more oxygen molecules, which assist in oxidizing the entire fuel, thus reducing the smoke emissions [55]. The smoke opacity of the blend at CRs 16:1, 17:1 and 18:1 was 62.2%, 57.2% and 511.6%, respectively, at full load. It was noted that the smoke opacity reduced with increasing CR because, as the CR increases, the combustion temperature also rises as a consequence of greater fuel atomization [15]. This results in reduced smoke opacity. At CR 18:1 at full load, the blend's smoke opacity was found to be the lowest at 51.6 ppm, and it was 23.44% lower than diesel at standard CR.

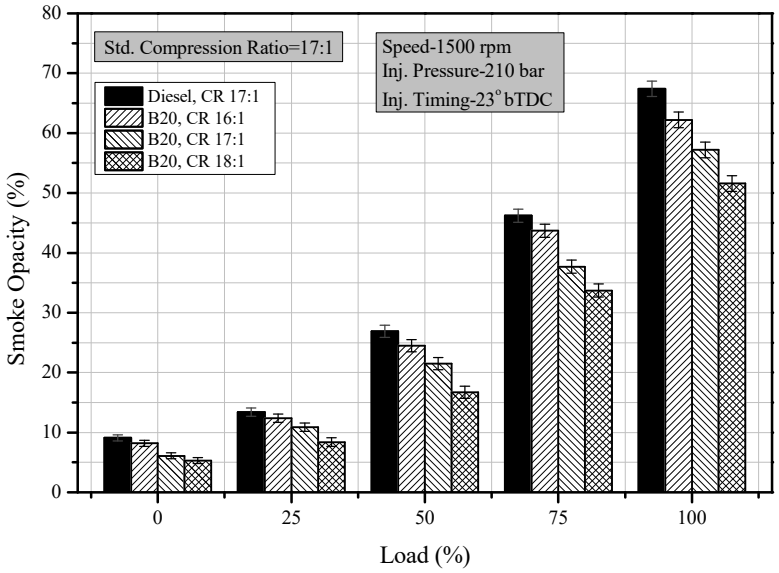

Figure 10. Smoke opacity vs. load at different CRs.

3.2.5. Comparative Analysis in Emissions

The percentage difference in emissions between the B20 blend at various CRs and diesel at standard CR and full load is illustrated in Figure 11. The B20 blend resulted in having lower CO emissions than diesel at all the CRs. They were 7.14%, 14.28% and 26.78% lower than diesel at CRs 16:1, 17:1 and 18:1, respectively. When compared to diesel, the blend's HC emissions were reduced by 10.76%, 16.92% and 36.76% at CRs 16:1, 17:1 and 18:1, respectively. Despite the decrease in HC and CO emissions, the blend's NO_x emissions rose in all CRs. The NO_x emissions at CR 16:1, 17:1 and 18:1 were 0.77%, 6.03% and 14.27% higher than diesel, respectively. The smoke opacity of the blend dropped at all CRs. At CRs 16:1, 17:1 and 18:1, the smoke opacity of the blend was 7.71%, 15.13% and 23.44% lower than diesel, respectively. The overall emissions decreased as the CR increased. The primary cause of the improvement in emissions is due to the shorter delay period at higher CRs, which improves the air density, in-cylinder temperature and fuel atomization. Increasing NO_x emissions was a consequence of high in-cylinder temperature and high oxygen concentration in the blend.

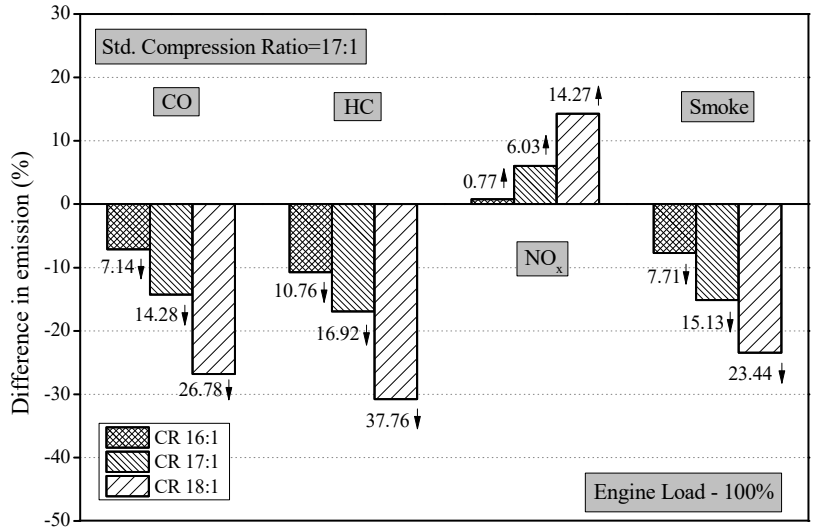

Figure 11. Percentage difference in B20 blend's emission at varying CRs to diesel at standard CR and full load.

3.3. Combustion Characteristics

3.3.1. Impact on In-Cylinder Pressure

The in-cylinder pressure (Cp) vs. crank angle (CA) diagram is to analyze the combustion behavior of an engine as it has a major impact on the engine characteristics [45]. Figure 12 displays the variations in Cp for the B20 blend and diesel at different CRs in response to crank angle while the engine is running at full load. The maximum in-cylinder pressure reached by the fuel in CI engines is most likely governed by the mass of fuel burnt during this period. At full load and standard CR, the highest Cp for diesel and the B20 blend were 59.45 bar at 367 °CA and 58.22 bar at 369 °CA, respectively. Due to the blend's increased viscosity and density, less fuel is built-up during the premixed combustion phase, therefore leading to lower peak cylinder pressure than diesel [54]. The maximum Cp for the blend at CRs 16:1, 17:1 and 18:1 was noted to be 55.85 bar at 367 °CA, 58.22 bar at 369 °CA and 65.94 bar at 368 °CA, respectively. The cylinder pressure increased with the greater CR as the intake temperature of the air rose in tandem with the CR, improving fuel atomization and resulting in a quicker combustion process [14]. Compared to the diesel's cylinder pressure at standard CR, the maximum cylinder pressure obtained by the blend improved by 10.91% when experimented with CR 18:1 at full load.

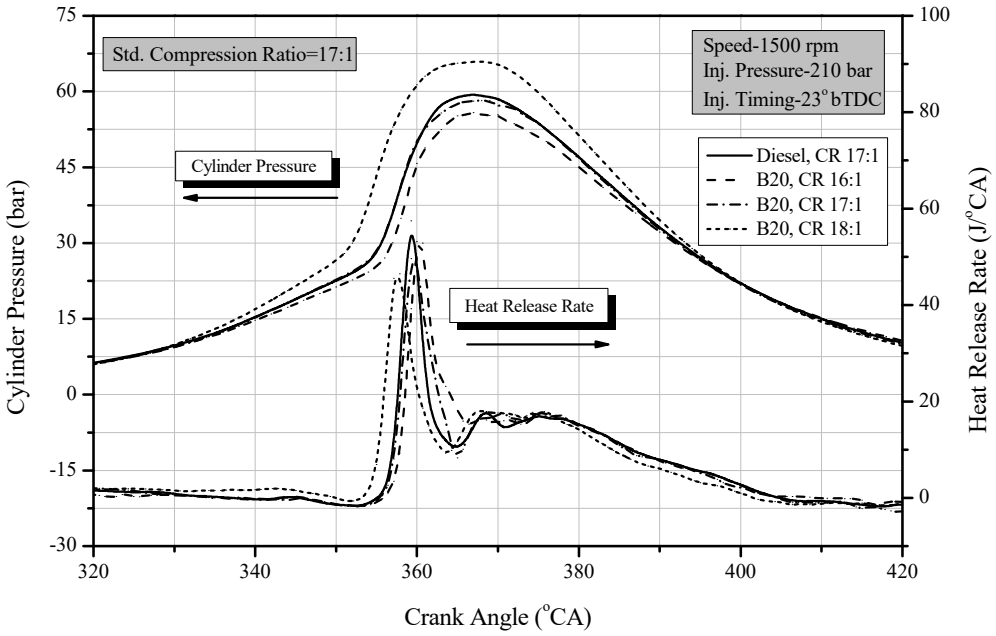

Figure 12. In-cylinder pressure and heat release rate vs. CA at different CRs.

3.3.2. Impact on Heat RELEASE rate

The heat release rate (HRR) is a viable approach to describe the combustion mechanism of a diesel engine [51]. Figure 12 also shows a comparison of HRR curves for diesel and B20 blend at various CRs in contrast to one another at full load. At standard CR, the maximum HRR for diesel and the B20 blend was determined to be 57.45 and 49.65 J/CA at full load, respectively. Diesel has a larger HRR than the blend due to its higher calorific value and longer ignition delay, allowing more fuel to collect in the combustion chamber [56]. The blend's HRR at CRs 16:1, 17:1 and 18:1 was 53.16, 49.65 and 46.47 J/CA. As illustrated in Figure 12 the maximum HRR falls as the engine compression ratio rises. This might be because the maximum in-cylinder temperature increases as the CR of the engine increases, hence increasing the rate of heat transfer inside the cylinder during combustion [57].

4. Conclusions

Tests were conducted to evaluate the characteristics of a VCR engine running with B20 blend of sea mango biodiesel at different CRs of 16:1, 17:1 and 18:1. There were two stages

to this study. The first stage includes the preparation of biodiesel and testing its properties. The second stage deals with the engine testing and its characteristics when fueled with B20 blend of sea mango biodiesel at different CRs. The test results of the B20 blend were then compared to that of diesel, which was operated at standard CR (17:1). The following are the findings of the experimental investigation:

- At standard CR, the BTE of the B20 blend was almost identical to diesel. Though the BTE of the B20 blend was lower at CR 16:1 and 17:1 than diesel, at CR 18:1, the BTE of the blend improved by 5.57%. The SFC and EGT also improved with higher CRs. At CR 18:1, the SFC was 6.25% lower than diesel, whereas the EGT was still 4% higher.
- The CO of the B20 blend was lower than diesel at all the CRs. At CR 18:1, the B20 blend resulted in having 26.78% lowered CO emissions than diesel. The HC of the B20 blend was also lower than diesel at all CRs. The B20 blend at CR 18:1 resulted in the lowest HC emissions, with 37.76% lower than diesel. Moreover, the NO_x emission was higher than diesel for the B20 blend at all the CRs. As the CRs lowered, the NO_x emission of the blend reduced. Diesel had the lowest NO_x emission of 1044 ppm at standard CR. The lowest NO_x level tested for the blend was 1052 ppm at CR 16:1, which was still 0.77% higher than diesel. The blend produced 14.27% higher NO_x emissions than diesel at CR 18:1. At all CRs, the B20 blend had lower smoke opacity values than diesel. The opacity of the smoke decreased with higher CRs. The least smoke opacity was 23.44% lower than diesel, obtained by the B20 blend at CR 18:1.
- The Cp and HRR of diesel and the blend were almost identical at standard CR. The peak cylinder pressure increased as the CR increased. At CR 18:1, the maximum Cp of the B20 blend was measured to be 65.94 bar. The HRR, on the other hand, decreased as the CR increased. The B20 blend had the least HRR of 46.47 J/CA at CR 18:1.

The current investigation could be concluded that the B20 blend of sea mango biodiesel may be a viable alternative to diesel fuel operated at CR of 18:1. In addition to the ability of sea mangos' high biodiesel production, its superior performance, emissions and combustion characteristics at greater compression ratios have made significant contributions to the success of this project. The increased NO_x emissions of the blend may be mitigated by using water emulsification or exhaust gas recirculation methods. Furthermore, the research may be broadened to evaluate the impact of additives added to sea mango biodiesel blends at different proportions, analyzing its engine characteristics.

Author Contributions: Conceptualization, R.R.R., A.J.S., R.Č. and M.E.; data curation, R.R.R.; formal analysis, R.R.R.; investigation, R.R.R.; methodology, R.R.R., A.J.S., R.Č. and M.E.; supervision, A.J.S. and R.Č.; visualization, R.R.R. and M.E.; writing—original draft, R.R.R. and A.J.S.; writing—review and editing, R.Č. and M.E. All authors have read and agreed to the published version of the manuscript.

Funding: This research received no external funding.

Institutional Review Board Statement: Not applicable.

Informed Consent Statement: Not applicable.

Data Availability Statement: The data presented in this study are available through email upon request to the corresponding author.

Conflicts of Interest: The authors declare no conflict of interest.

Abbreviations

VCR	Variable Compression Ratio
CR	Compression Ratio
CI	Combustion Ignition
B20	20% Sea Mango Biodiesel + 80% Diesel
IBDC	Indian Biodiesel Corporation

IEA	International Energy Agency
BTE	Brake Thermal Efficiency
SFC	Specific Fuel Consumption
EGT	Exhaust Gas Temperature
EGR	Exhaust Gas Recirculation
CO	Carbon monoxide
HC	Hydrocarbon
NO_x	Oxides of Nitrogen
Cp	In-cylinder pressure
HRR	Heat Release Rate

References

1. Shrivastava, P.; Salam, S.; Verma, T.N.; Samuel, O.D. Experimental and empirical analysis of an IC engine operating with ternary blends of diesel, karanja and roselle biodiesel. *Fuel* **2019**, *262*, 116608. [CrossRef]
2. Hasan, M.; Rahman, M. Performance and emission characteristics of biodiesel–diesel blend and environmental and economic impacts of biodiesel production: A review. *Renew. Sustain. Energy Rev.* **2017**, *74*, 938–948. [CrossRef]
3. Helwani, Z.; Aziz, N.; Bakar, M.; Mukhtar, H.; Kim, J.; Othman, M. Conversion of Jatropha curcas oil into biodiesel using re-crystallized hydrotalcite. *Energy Convers. Manag.* **2013**, *73*, 128–134. [CrossRef]
4. Kamari, M.L.; Maleki, A.; Nazari, M.A.; Sadeghi, M.; Rosen, M.A.; Pourfayaz, F. Assessment of a biomass-based polygeneration plant for combined power, heat, bioethanol and biogas. *Appl. Therm. Eng.* **2021**, *198*, 117425. [CrossRef]
5. Nazari, M.A.; Alavi, M.F.; Salem, M.; Assad, M.E.H. Utilization of hydrogen in gas turbines: A comprehensive review. *Int. J. Low-Carbon Technol.* **2022**, *17*, 513–519. [CrossRef]
6. Gupta, K.; Kalita, K.; Ghadai, R.; Ramachandran, M.; Gao, X.-Z. Machine Learning-Based Predictive Modelling of Biodiesel Production—A Comparative Perspective. *Energies* **2021**, *14*, 1122. [CrossRef]
7. Kalita, P.; Basumatary, B.; Saikia, P.; Das, B.; Basumatary, S. Biodiesel as renewable biofuel produced via enzyme-based catalyzed transesterification. *Energy Nexus* **2022**, *6*, 10008. [CrossRef]
8. Mota, G.F.; de Sousa, I.G.; de Oliveira, A.L.B.; Cavalcante, A.L.G.; Moreira, K.d.S.; Cavalcante, F.T.T.; Souza, J.E.D.S.; Falcão, R.d.A.; Rocha, T.G.; Valério, R.B.R.; et al. Biodiesel production from microalgae using lipase-based catalysts: Current challenges and prospects. *Algal Res.* **2022**, *62*, 102616. [CrossRef]
9. Babadi, A.A.; Rahmati, S.; Fakhlaei, R.; Barati, B.; Wang, S.; Doherty, W.; Ostrikov, K. Emerging technologies for biodiesel production: Processes, challenges, and opportunities. *Biomass- Bioenergy* **2022**, *163*. [CrossRef]
10. Andreo-Martínez, P.; Ortiz-Martínez, V.M.; Salar-García, M.J.; Veiga-Del-Baño, J.M.; Chica, A.; Quesada-Medina, J. Waste animal fats as feedstock for biodiesel production using non-catalytic supercritical alcohol transesterification: A perspective by the PRISMA methodology. *Energy Sustain. Dev.* **2022**, *69*, 150–163. [CrossRef]
11. Fadhil, A.B.; Al-Tikrity, E.T.; Albadree, M.A. Biodiesel production from mixed non-edible oils, castor seed oil and waste fish oil. *Fuel* **2017**, *210*, 721–728. [CrossRef]
12. Rao, B.S.; Selvam, M.A.J. Experimental invistigation on di diesel engine fueled with datura seed biodiesel. *Int. J. Mech. Eng. Technol.* **2018**, *9*, 285–292.
13. Dugala, N.S.; Goindi, G.S.; Sharma, A. Experimental investigations on the performance and emissions characteristics of dual biodiesel blends on a varying compression ratio diesel engine. *SN Appl. Sci.* **2021**, *3*, 1–17. [CrossRef]
14. Shaik, A.A.; Reddy, S.R.; Raju, V.D.; Govindarajan, M. Combined influence of compression ratio and EGR on diverse characteristics of a research diesel engine fueled with waste mango seed biodiesel blend. *Energy Sources Part A Recover. Util. Environ. Eff.* **2020**, 1–24. [CrossRef]
15. Rosha, P.; Mohapatra, S.K.; Mahla, S.K.; Cho, H.; Chauhan, B.S.; Dhir, A. Effect of compression ratio on combustion, performance, and emission characteristics of compression ignition engine fueled with palm (B20) biodiesel blend. *Energy* **2019**, *178*, 676–684. [CrossRef]
16. Suresh, M.; Jawahar, C.; Renish, R.; Malmquist, A. Performance evaluation and emission characteristics of variable compression ratio diesel engine using Argemone Mexicana biodiesel. *Energy Sources Part A Recover. Util. Environ. Eff.* **2019**, *43*, 1511–1523. [CrossRef]
17. Sivaramakrishnan, K. Investigation on performance and emission characteristics of a variable compression multi fuel engine fuelled with Karanja biodiesel–diesel blend. *Egypt. J. Pet.* **2018**, *27*, 177–186. [CrossRef]
18. Datta, A.; Mandal, B.K. An experimental investigation on the performance, combustion and emission characteristics of a variable compression ratio diesel engine using diesel and palm stearin methyl ester. *Clean Technol. Environ. Policy* **2017**, *19*, 1297–1312. [CrossRef]
19. Vasudeva, M.; Sharma, S.; Mohapatra, S.K.; Kundu, K. Performance and exhaust emission characteristics of variable compression ratio diesel engine fuelled with esters of crude rice bran oil. *SpringerPlus* **2016**, *5*, 1–13. [CrossRef]
20. Bora, B.J.; Saha, U.K. Experimental evaluation of a rice bran biodiesel-biogas run dual fuel diesel engine at varying compression ratios. *Renew. Energy* **2016**, *87*, 782–790. [CrossRef]

21. Sharma, A.; Murugan, S. Potential for using a tyre pyrolysis oil-biodiesel blend in a diesel engine at different compression ratios. *Energy Convers. Manag.* **2015**, *93*, 289–297. [CrossRef]
22. Bora, B.J.; Saha, U.K.; Chatterjee, S.; Veer, V. Effect of compression ratio on performance, combustion and emission characteristics of a dual fuel diesel engine run on raw biogas. *Energy Convers. Manag.* **2014**, *87*, 1000–1009. [CrossRef]
23. El_Kassaby, M.; Nemit_Allah, M.A. Studying the effect of compression ratio on an engine fueled with waste oil produced biodiesel/diesel fuel. *Alex. Eng. J.* **2013**, *52*, 1–11. [CrossRef]
24. Muralidharan, K.; Vasudevan, D. Performance, emission and combustion characteristics of a variable compression ratio engine using methyl esters of waste cooking oil and diesel blends. *Appl. Energy* **2011**, *88*, 3959–3968. [CrossRef]
25. Suresh, M.; Jawahar, C.; Richard, A. A review on biodiesel production, combustion, performance, and emission characteristics of non-edible oils in variable compression ratio diesel engine using biodiesel and its blends. *Renew. Sustain. Energy Rev.* **2018**, *92*, 38–49. [CrossRef]
26. Fayad, M.A. Effect of renewable fuel and injection strategies on combustion characteristics and gaseous emissions in diesel engines. *Energy Sources Part A Recover. Util. Environ. Eff.* **2019**, *42*, 460–470. [CrossRef]
27. Fattah, I.R.; Masjuki, H.; Kalam, M.; Wakil, M.; Rashedul, H.; Abedin, M. Performance and emission characteristics of a CI engine fueled with Cocos nucifera and Jatropha curcas B20 blends accompanying antioxidants. *Ind. Crop. Prod.* **2014**, *57*, 132–140. [CrossRef]
28. Narayanasamy, B.; Jeyakumar, N. Performance and emission analysis of methyl ester of Azolla algae with TiO_2 Nano additive for diesel engine. *Energy Sources Part A Recover. Util. Environ. Eff.* **2018**, *41*, 1434–1445. [CrossRef]
29. Venu, H.; Appavu, P. Experimental studies on the influence of zirconium nanoparticle on biodiesel–diesel fuel blend in CI engine. *Int. J. Ambient Energy* **2019**, *42*, 1588–1594. [CrossRef]
30. Channappagoudra, M.; Ramesh, K.; Manavendra, G. Bio-ethanol additive effect on direct injection diesel engine performance, emission and combustion characteristics—An experimental examination. *Int. J. Ambient Energy* **2018**, *41*, 1342–1351. [CrossRef]
31. Balaji, S.; Saravanan, R.; Kapilan, N. Influence of Propyl gallate antioxidant on performance and emissions of a compression ignition engine fueled with Madhuca Indica B20 ester blends. *Energy Sources Part A Recover. Util. Environ. Eff.* **2019**, *43*, 2197–2209. [CrossRef]
32. Chiriac, R.; Apostolescu, N. Emissions of a diesel engine using B20 and effects of hydrogen addition. *Int. J. Hydrogen Energy* **2013**, *38*, 13453–13462. [CrossRef]
33. Bari, S. Performance, combustion and emission tests of a metro-bus running on biodiesel-ULSD blended (B20) fuel. *Appl. Energy* **2014**, *124*, 35–43. [CrossRef]
34. Mubarak, M.; Shaija, A.; Suchithra, T. Experimental evaluation of Salvinia molesta oil biodiesel/diesel blends fuel on combustion, performance and emission analysis of diesel engine. *Fuel* **2020**, *287*, 119526. [CrossRef]
35. Soni, A.K.; Kumar, S.; Pandey, M. Performance Comparison of Microalgae Biodiesel Blends with Petro–Diesel on Variable Compression Ratio Engine. *J. Inst. Eng. (India) Ser. E* **2020**, *103*, 53–63. [CrossRef]
36. Renish, R.R.; Selvam, M.A.J. A critical review on production process, physicochemical properties, performance and emission characteristics of sea mango biodiesel-diesel blends. *Mater. Today Proc.* **2021**, *44*, 2600–2605. [CrossRef]
37. Kansedo, J.; Lee, K.T.; Bhatia, S. Cerbera odollam (sea mango) oil as a promising non-edible feedstock for biodiesel production. *Fuel* **2009**, *88*, 1148–1150. [CrossRef]
38. Kumar, V.; Kalita, K.; Madhu, S.; Ragavendran, U.; Gao, X.-Z. A Hybrid Genetic Programming–Gray Wolf Optimizer Approach for Process Optimization of Biodiesel Production. *Processes* **2021**, *9*, 442. [CrossRef]
39. Lie, J.; Rizkiana, M.B.; Soetaredjo, F.E.; Ju, Y.-H.; Ismadji, S. Production of biodiesel from sea mango (Cerbera odollam) seed using in situ subcritical methanol–water under a non-catalytic process. *Int. J. Ind. Chem.* **2018**, *9*, 53–59. [CrossRef]
40. Gaillard, Y.; Krishnamoorthy, A.; Bevalot, F. Cerbera odollam: A 'suicide tree' and cause of death in the state of Kerala, India. *J. Ethnopharmacol.* **2004**, *95*, 123–126. [CrossRef]
41. Ramos, M.; Dias, A.P.S.; Puna, J.F.; Gomes, J.; Bordado, J.C. Biodiesel Production Processes and Sustainable Raw Materials. *Energies* **2019**, *12*, 4408. [CrossRef]
42. Jaichandar, S.; Annamalai, K. Effects of open combustion chamber geometries on the performance of pongamia biodiesel in a DI diesel engine. *Fuel* **2012**, *98*, 272–279. [CrossRef]
43. Das, M.; Sarkar, M.; Datta, A.; Santra, A.K. An experimental study on the combustion, performance and emission characteristics of a diesel engine fuelled with diesel-castor oil biodiesel blends. *Renew. Energy* **2017**, *119*, 174–184. [CrossRef]
44. Jindal, S.; Nandwana, B.; Rathore, N.; Vashistha, V. Experimental investigation of the effect of compression ratio and injection pressure in a direct injection diesel engine running on Jatropha methyl ester. *Appl. Therm. Eng.* **2010**, *30*, 442–448. [CrossRef]
45. Hariram, V.; Shangar, R.V. Influence of compression ratio on combustion and performance characteristics of direct injection compression ignition engine. *Alex. Eng. J.* **2015**, *54*, 807–814. [CrossRef]
46. Saravanan, A.; Murugan, M.; Reddy, M.S.; Parida, S. Performance and emission characteristics of variable compression ratio CI engine fueled with dual biodiesel blends of Rapeseed and Mahua. *Fuel* **2019**, *263*, 116751. [CrossRef]
47. Sayin, C.; Gumus, M. Impact of compression ratio and injection parameters on the performance and emissions of a DI diesel engine fueled with biodiesel-blended diesel fuel. *Appl. Therm. Eng.* **2011**, *31*, 3182–3188. [CrossRef]
48. Gad, M.; Kamel, B.M.; Badruddin, I.A. Improving the diesel engine performance, emissions and combustion characteristics using biodiesel with carbon nanomaterials. *Fuel* **2020**, *288*, 119665. [CrossRef]

49. Choudhary, K.D.; Nayyar, A.; Dasgupta, M. Effect of compression ratio on combustion and emission characteristics of C.I. Engine operated with acetylene in conjunction with diesel fuel. *Fuel* **2018**, *214*, 489–496. [CrossRef]
50. Gharehghani, A.; Hosseini, R.; Mirsalim, M.; Yusaf, T.F. A computational study of operating range extension in a natural gas SI engine with the use of hydrogen. *Int. J. Hydrogen Energy* **2015**, *40*, 5966–5975. [CrossRef]
51. Ruhul, A.; Kalam, M.; Masjuki, H.; Shahir, S.; Alabdulkarem, A.; Teoh, Y.; How, H.; Reham, S. Evaluating combustion, performance and emission characteristics of Millettia pinnata and Croton megalocarpus biodiesel blends in a diesel engine. *Energy* **2017**, *141*, 2362–2376. [CrossRef]
52. More, G.V.; Koli, S.R.; Rao, Y.V.H.; Prasad, P.I.; Rao, B.N. Effect of compression ratio on compression ignition engine with RUCO biodiesel/ diethyl ether/ diesel fuel blends. *Energy Sources Part A Recover. Util. Environ. Eff.* **2020**, 1–20. [CrossRef]
53. Gugulothu, S.K. Retracted: Experimental investigation of the influence of combustion chambers and compression ratio on the performance and emission characteristics of diesel engine. *Heat Transf.* **2020**, *50*, 1021. [CrossRef]
54. Balamurugan, T.; Arun, A.; Sathishkumar, G. Biodiesel derived from corn oil—A fuel substitute for diesel. *Renew. Sustain. Energy Rev.* **2018**, *94*, 772–778. [CrossRef]
55. Abed, K.; Gad, M.; El Morsi, A.; Sayed, M.; Abu Elyazeed, S. Effect of biodiesel fuels on diesel engine emissions. *Egypt. J. Pet.* **2019**, *28*, 183–188. [CrossRef]
56. Dash, S.K.; Lingfa, P.; Chavan, S.B. Combustion analysis of a single cylinder variable compression ratio small size agricultural DI diesel engine run by Nahar biodiesel and its diesel blends. *Energy Sources Part A Recover. Util. Environ. Eff.* **2019**, *42*, 1681–1690. [CrossRef]
57. Ibrahim, A.; El-Adawy, M.; El-Kassaby, M.M. The Impact of Changing the Compression Ratio on the Performance of an Engine fueled by Biodiesel Blends. *Energy Technol.* **2013**, *1*, 395–404. [CrossRef]